A Low-Voltage Drive, Piston-motion Micromirror Array with 94% Fill Factor

Elizabeth Murray[1†], Nathan Tessema Ersaro[1†], Cem Yalcin[1], Munkyu Kang[1], Leyla Kabuli[1], Laura Waller[1], Rikky Muller[1,2*]
[1]Department of Electrical Engineering and Computer Sciences, University of California, Berkeley, [2]Weill Neurohub Berkeley, CA, USA
[†]Equally Credited Authors, [*]rikky@berkeley.edu

2025 International Conference on Optical MEMS and Nanophotonics (OMN) | 979-8-3315-9922-5/25/$31.00 ©2025 IEEE | DOI: 10.1109/OMN65869.2025.11126011

***Abstract*—We present an electrostatically-actuated, piston-motion micromirror array for applications in 3D point scanning and holography. Individual mirror pixels can be controlled with low-voltage analog drive over a 300 nm actuation range and achieve 10-90% mechanical settling times of less than 160 µs. An efficient pixel tiling scheme that allows adjacent mirrors to share the anchors of the suspension structure results in a 94% fill factor for high optical efficiency.**

***Index Terms*—micromirror, Poly-MUMPS, holography**

I. Introduction

Micromirrors and micromirror arrays (MMAs) are a popular technology for beam steering and lateral point scanning with applications in optical switching [1], microscopy [2], and displays [3]. However, high-speed ($\geq$ 5 kHz) holographic projection for emerging applications such as optical neural interfaces [4] and AR/VR near-eye displays [5] remains a challenge. Commercialized tip/tilt MMAs such as Texas Instruments' (TI) DMDs [6] can achieve kHz refresh rates but are unable to provide the phase control necessary for efficient holographic projection. Current 3D projection systems thus typically rely on slow-settling liquid-crystal-based spatial light modulators (SLMs) [7] with refresh rates limited to around 500 Hz. Piston-motion MMAs have emerged as a promising solution, achieving pixel-level phase control at kHz speeds [8], but have generally been limited to prototypes in specialized processes [9] [10]. In this work, we present a design that can be fabricated through a standard MEMS foundry service with only a few modifications. The resulting piston-motion MMA optimizes for optical performance and scalability while enabling continued low-cost development.

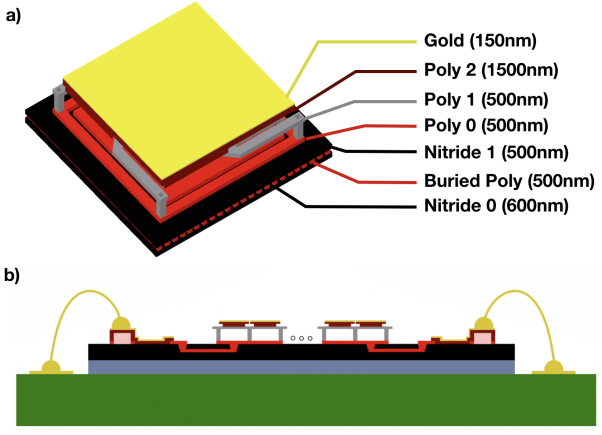

Fig. 1. a) Pixel stackup b) Cross section of chip-on-board assembly of micromirror array. Illustrations not-to-scale.

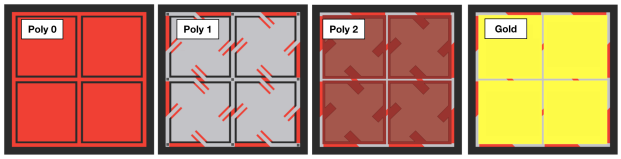

Fig. 2. Pixel tiling scheme and stackup. Vias through the oxide layer separating Poly 0 from Poly 1 are shown in dark gray on the Poly 1 layer. Vias separating Poly 1 from Poly 2 are shown in a transparent highlight on the Poly 2 layer.

For discrete pixel arrays, diffraction efficiency is limited to the square of the fill factor [11], and is further reduced by non-planarity in the mirror structure. Overall optical efficiency also degrades if reflectivity is low. Efficiency requirements are thus driving arrays towards highly-reflective, closely-packed, planar mirror geometries. Low power consumption is also critical for scaling MMAs to higher pixel counts. In particular, low-voltage drive facilitates the compact integration of CMOS drive electronics at scale.

To optimize for these considerations, we present a 94% fill factor, 10V drive, piston-motion MMA design. When driven with a custom ASIC, micromirrors can be controlled over an actuation range of 300 nm with 10-90% settling times of under 160 µs.

II. Micromirror Design and Fabrication

The 70 µm-pitch mircromirror array was designed and fabricated in a modified Poly-MUMPS surface micromachining process, with the layer stackup and geometry of an individual pixel shown in Fig. 1a. The core mirror structure consists of three LPCVD polysilicon structural layers and an evaporated gold layer for reflectivity. The mirror is actuated through electrostatic drive, with the top plate stackup of each mirror grounded and each bottom plate connected to drive electronics through via openings in the nitride film to traces in a buried polysilicon routing layer. While this routing can be designed to access each mirror individually, it also gives the flexibility to connect mirrors in groups for specific optical tasks (e.g. rings for focus tuning, columns for beam steering). Top plates of all mirrors in the array are grounded through the anchoring of Poly 1 suspension structures to a grid-shaped ground network

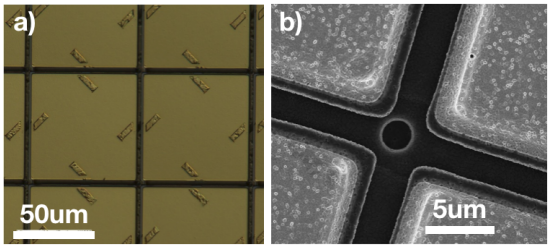

Fig. 3. a) Optical microscopy image of micromirror pixels. b) Scanning electron microscopy image of the Poly 1 anchor shared among micromirrors.

patterned in Poly 0 (Fig. 2). Adjacent mirrors thus share anchor points, allowing the mirrors to be closely packed for high fill factor. In the areas of the bottom electrodes, Poly 0 and Poly 1 are separated by a 2 µm thick sacrificial Oxide 1, and in the areas above the suspension beams, Poly 2 and Poly 1 are separated by a 750 nm thick Oxide 2. After release, this architecture prevents shorting due to electrostatic pull-in at high voltages as the Poly 2 mirror body will be mechanically stopped through contact with the Poly 1 anchor posts.

III. Characterization and Performance

An array with the micromirrors connected in concentric rings through the buried polysilicon routing layer was evaluated. Images of the fabricated micromirror pixels from this array are shown in Fig. 3. The surface profile of a representative mirror, measured under a digital holographic microscope (LynceeTec DHM R2100), is shown in Fig. 4b. The bowing after release of the sacrificial oxide layers was less than 50 nm over the 96 µm mirror diagonal, demonstrating that the thick Poly 2 layer was sufficient to reinforce the mirror body against the residual stress of the evaporated gold coating. The observed dip in the topography at the center of each pixel is due to the propagation of the via connecting the bottom electrode to the buried polysilicon layer.

The transduction curves of 69 mirrors in the third ring of the array were measured with the DHM (Fig. 4c). Fitting the mean curve to the general form of the analytical solution to parallel plate actuation, $V = \sqrt{a\Delta x(b - \Delta x)}$, resulted in an inferred gap height of $b = 2.13\mu m$, consistent with the thickness of Oxide 1. No shorting due to electrostatic pull-in was observed, validating the effectiveness of the mechanical gap stops. The dynamic response of these mirrors was characterized with

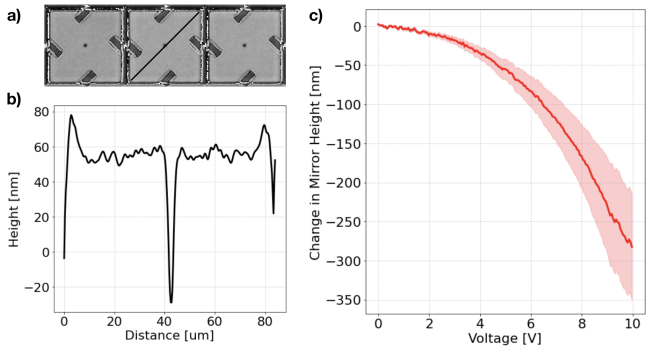

Fig. 4. a) Phase image of individual pixels. b) Mirror height measurement corresponding to diagonal line in a). c) Average displacement over 69 mirrors in a ring and +/- standard deviation.

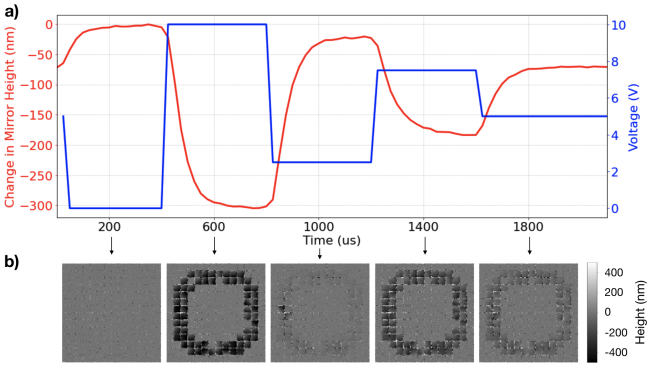

Fig. 5. a) Average micromirror displacement in response to five different voltage steps. b) Phase images at 400 µs intervals.

the DHM's stroboscopic module (Fig. 5a), and the change in pixel height relative to the array's resting height across the microscope's field of view is shown in Fig. 5b. The 10-90% settling times ranged from 110 µs to 156 µs for five different step sizes, covering an actuation range of 300 nm.

We successfully demonstrate a low-voltage, high fill factor piston-motion MMA fabricated in a modified Poly-MUMPS process. Sub-200 µs pixel speeds represent a 10x improvement over LCoS-based SLMs, and our design demonstrates the viability of low-cost piston-motion MMA development in a standard MEMS process.

Acknowledgment

The authors thank Coventorware for simulation tools and Sarika Madhvapathy and Yichen Liu for device imaging. This work was supported by NIH National Institute of Neurological Disorders and Stroke and the Weill Neurohub.

References

[1] M. Yano, et al., "Optical MEMS for photonic switching-compact and stable optical crossconnect switches for simple, fast, and flexible wavelength applications in recent photonic networks," IEEE Journal of Selected Topics in Quantum Electronics, vol. 11, no. 2, pp. 383-394, 2005.

[2] H. Ra, et al., "Two-Dimensional MEMS Scanner for Dual-Axes Confocal Microscopy," Journal of Microelectromechanical Systems, vol. 16, no. 4, pp. 969-976, 2007.

[3] C. -d. Liao, et al., "The Evolution of MEMS Displays," IEEE Transactions on Industrial Electronics, vol. 56, no. 4, pp. 1057-1065, 2009.

[4] N.T. Ersaro, et al., "The future of brain–machine interfaces is optical," Nature Electronics 6, 96–98, 2023.

[5] A. Maimone, et al., "Holographic Near-Eye Displays for Virtual and Augmented Reality," ACM Trans. Graph. 36.4, 2017.

[6] B. Lee, "DMD 101: Introduction to Digital Micromirror Device (DMD)," 2013.

[7] Y. Yang et al., "A review of liquid crystal spatial light modulators: devices and applications," Opto-Electron Sci 2, 230026, 2023.

[8] N. T. Ersumo, et al., "A micromirror array with annular partitioning for high-speed random-access axial focusing," Light Sci Appl 9, 183, 2020.

[9] T.A. Bartlett, et al., "Recent advances in the development of the Texas Instruments phase-only microelectromechanical systems (MEMS) spatial light modulator," Emerging Digital Micromirror Device Based Systems and Applications XIII 11698, pp. 103–116, 2021.

[10] S. Francés González, et al. "Characterization of MEMS piston mirror arrays with comb drive actuator," Proc. SPIE 12899, MOEMS and Miniaturized Systems XXIII, 128990D, 2024.

[11] V. Arrizón, et al. "Implementation of Fourier array illuminators using pixelated SLM: efficiency limitations," Optics Communications, vol. 160, no. 4–6, pp. 207-213, 1999.